

---

# Vibrational and electronic properties of $\text{Al}_{12}\text{M}$ ( $\text{M}=\text{Cu}, \text{Zn}$ ) clusters: DFT calculations

P. L. Rodríguez-Kessler<sup>1,\*</sup>

1 Centro de Investigaciones en Óptica A.C., Loma del Bosque 115, Lomas del Campestre, Leon, 37150, Guanajuato, Mexico \*plkessler@cio.mx

## Abstract

In this work, the vibrational and electronic properties of  $\text{Al}_{12}\text{M}$  ( $\text{Zn}, \text{Cu}$ ) clusters are investigated using density functional theory (DFT) calculations. The results indicate that the clusters favor low-spin states when evaluated with three different functionals: PBE, PBE0, and TPSSh. Additionally, the doped clusters exhibit lower ionization energy and electron affinity compared to the neutral  $\text{Al}_{13}$  cluster. The density of states show a higher degree of hybridization in  $\text{Al}_{12}\text{Cu}$  compared to  $\text{Al}_{12}\text{Zn}$ .

## Introduction

Aluminum clusters and nanoparticles have garnered significant interest from researchers due to their wide range of potential applications. In particular, aluminium-based nanoclusters have shown promising properties for clean energy applications. [1–3] The growth mechanism, electronic properties and spectra of aluminum clusters with 3–20 atoms has been studied by Tan et al. [4] They revealed that the  $\text{Al}_7^+$  and  $\text{Al}_{13}^-$  clusters exhibit very high stability and a large energy gap, and can be regarded as superatoms. Moreover, the absorption spectra of neutral aluminum clusters have been simulated and compared with experimental findings. [5] The  $\text{Al}_{13}$  cluster, in particular, is widely studied due to its superatom characteristics in the anionic state. Additionally, the icosahedral structure of  $\text{Al}_{13}$  makes it an attractive system with a well-defined geometry. [6] In order to enhance the catalytic properties through specific applications, a study of both exohedral and endohedral doping on the  $\text{Al}_{13}$  cluster has been conducted. For example, endohedral and exohedral magnesium-doped aluminum clusters were evaluated for their hydrogen adsorption properties. [7] Vanbuel et al. evaluated the  $\text{H}_2$  chemisorption on  $\text{Al}_n\text{Rh}^{2+}$  ( $n=10-13$ ) clusters and found that for  $n=10$  and  $11$ , a single  $\text{H}_2$  molecule binds dissociatively, whereas for  $n=12$  and  $13$ , it adsorbs molecularly. [8] Although many studies have evaluated the hydrogen adsorption properties of transition metal-doped Al clusters, only a few have examined their catalytic activities, and further progress in this area is still needed. [9] Recently, Samudre et al. investigated the endohedral doping of X atoms ( $X = \text{Ti}, \text{V}, \text{Fe}, \text{Co}, \text{Ni}, \text{Cu}, \text{Zn}, \text{Y}, \text{Mo}, \text{Ru}, \text{Rh}, \text{and W}$ ) in the  $\text{Al}_{13}$  cluster and revealed that only  $\text{Al}_{12}\text{Zn}$  and  $\text{Al}_{12}\text{Cu}$  are thermally stable endohedral clusters, according to BOMD simulation results. [10] However, further descriptive parameters of the clusters have not been evaluated so far. In this brief preprint, we investigate the vibrational and electronic properties of endohedral  $\text{Al}_{12}\text{Zn}$  and  $\text{Al}_{12}\text{Cu}$  clusters. The doped clusters show lower ionization energy and electron affinity compared to the neutral  $\text{Al}_{13}$  cluster. The density of states show a higher degree of hybridization in  $\text{Al}_{12}\text{Cu}$  compared to  $\text{Al}_{12}\text{Zn}$ .

## Materials and Methods

The calculations in this study utilize density functional theory (DFT) as implemented in the Orca quantum chemistry package. [11]. The Exchange and correlation energies are addressed using various functionals, including the GGA (PBE), [12] meta-GGA (TPSS) [13] and hybrid (PBE0) [14] in conjunction with the Def2-TZVP basis set. [15] Atomic positions are self-consistently relaxed through a Quasi-Newton method employing the BFGS algorithm. The SCF convergence criteria for geometry optimizations are achieved when the total energy difference is smaller than  $10^{-8}$  au, by using the TightSCF keyword in the input. The Van der Waals interactions are included in the exchange-correlation functionals with empirical dispersion corrections of Grimme DFT-D3(BJ). The total density of states (DOS) and partial density of states (PDOS) for clusters and complexes were obtained by using the Multiwfn program. [16]

## Results

The structure models for representing the  $\text{Al}_{12}\text{M}$  ( $\text{M}=\text{Cu}, \text{Zn}$ ) clusters are shown in Figure 1. The results show that the clusters favor the endohedral doping, however, we found that for  $\text{Al}_{12}\text{Cu}$  the low-spin state (doublet) is favored over the quartet state, which is in contrast with the report of Samudre et al. [10] We have further confirmed the results by using three different functionals (Table 1). The PBE and PBE0 functionals favor the doublet and singlet states for  $\text{Al}_{12}\text{Cu}$  and  $\text{Al}_{12}\text{Zn}$  clusters, while the TPSSh functional favor the doublet and singlet states by 0.001 eV and 0.04 eV of the total energy for the  $\text{Al}_{12}\text{Cu}$  and  $\text{Al}_{12}\text{Zn}$  clusters, respectively.

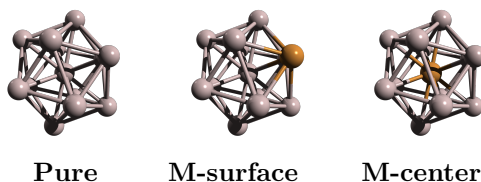


**Figure 1.** Representative icosahedral structures for  $\text{Al}_{13}$  and  $\text{Al}_{12}\text{M}$  clusters.

**Table 1.** Relative energies (in eV) of the lowest energy structures of  $\text{Al}_{12}\text{M}$  ( $\text{Cu}, \text{Zn}$ ) clusters computed at different DFT levels. Representative values on the spin multiplicity ( $S_M$ ) are given.

Label	$S_M$	PBE	PBE0	TPSSh
<b><math>\text{Al}_{12}\text{Zn}</math></b>	1	0.00	0.00	0.00
<b><math>\text{Al}_{12}\text{Cu}^a</math></b>	2	0.00	0.00	0.00
<b><math>\text{Al}_{12}\text{Zn}</math></b>	3	0.10	0.05	0.04
<b><math>\text{Al}_{12}\text{Cu}^b</math></b>	4	0.17	0.03	0.00

<sup>a</sup>This work.

<sup>b</sup>Ref.10

To identify the fingerprints of the  $\text{Al}_{12}\text{Cu}$  and  $\text{Al}_{12}\text{Zn}$  clusters, we have calculated the infrared (IR) spectra, which serve as a guide for future experimental studies when become available. [17, 18] The characteristic peak for  $\text{Al}_{12}\text{Cu}$  is found at  $180.02 \text{ cm}^{-1}$ , while for  $\text{Al}_{12}\text{Zn}$  is found at  $190.14 \text{ cm}^{-1}$  (Figure 2). The lowest and highest vibrational frequencies for  $\text{Al}_{12}\text{Cu}$  are  $54.22\text{-}305.41 \text{ cm}^{-1}$ , while for  $\text{Al}_{12}\text{Zn}$  are  $49.59\text{-}321.09 \text{ cm}^{-1}$ , respectively,

denoting a narrow range of their vibrational spectra. The representative vibrational modes of the  $\text{Al}_{12}\text{Cu}$  cluster primarily correspond to anti-symmetric stretching, [19] as shown in Figure 3.

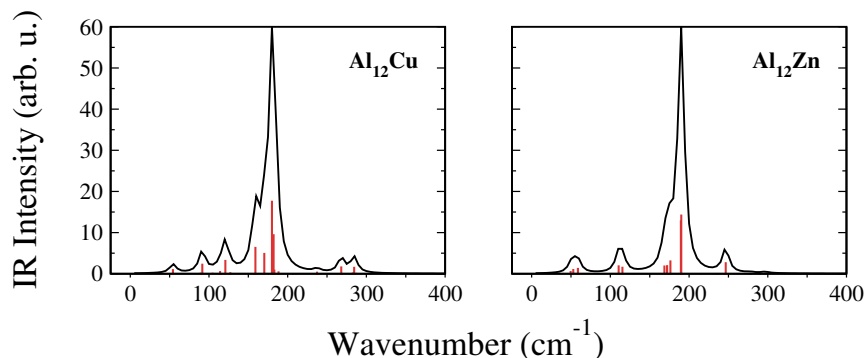


**Figure 2.** IR spectra for  $\text{Al}_{12}\text{Cu}$  and  $\text{Al}_{12}\text{Zn}$  clusters obtained at the PBE0/Def2-TZVP level.

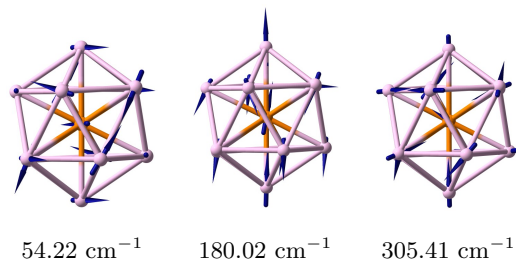


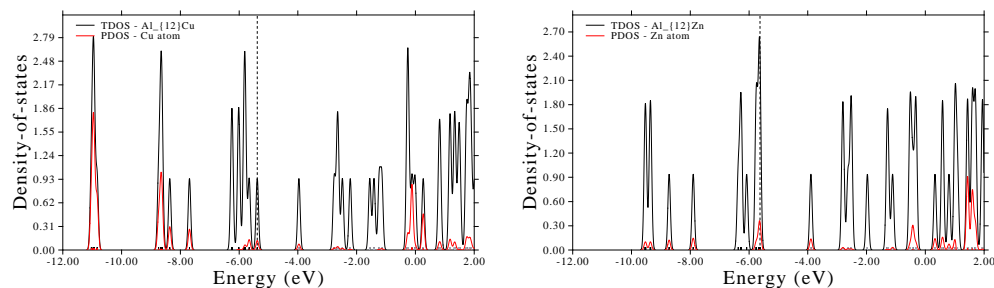
**Figure 3.** Representative vibrational modes for the  $\text{Al}_{12}\text{Cu}$  cluster.

The ionization energy (IP) and electron affinity (EA) are key physical parameters that indicate the electronic stability of clusters. The calculated values are presented in Table 2, while their formulas and definitions can be found elsewhere. [20–27] The results show that the  $\text{Al}_{12}\text{M}$  ( $\text{M}=\text{Cu}, \text{Zn}$ ) clusters have smaller IP values compared to the neutral  $\text{Al}_{13}$  cluster, suggesting an increase in reactivity.  $\text{Al}_{12}\text{Zn}$  shows the smaller EA value, followed by  $\text{Al}_{12}\text{Cu}$  and  $\text{Al}_{13}$ . The chemical hardness ( $\eta$ ) for  $\text{Al}_{12}\text{M}$  ( $\text{M}=\text{Cu}, \text{Zn}$ ) clusters show similar values compared to the bare  $\text{Al}_{13}$  clusters, while the chemical potential ( $\mu$ ) also showed a small reduction for the doped clusters. Moreover, the structures of the clusters exhibited only one rotational axis, consistent with  $\text{C}_1$  symmetry. The electronic states are  $^2\text{A}$  and  $^1\text{A}$  for the  $\text{Al}_{12}\text{Cu}$  and  $\text{Al}_{12}\text{Zn}$  clusters, respectively.

**Table 2.** The symmetry point group, electronic state, ionization energy, electron affinity, chemical hardness and chemical potential of  $\text{Al}_{12}\text{M}$  ( $\text{M}=\text{Cu}, \text{Zn}$ ) and  $\text{Al}_{13}$  clusters. The results are calculated at the PBE0 level in conjunction with the Def2-TZVP basis set. The energy is given in eV.

Cluster	Sym	$E_{state}$	IP	EA	$\eta$	$\mu$
$\text{Al}_{12}\text{Cu}^b$	$\text{C}_1$	$^2\text{A}$	6.64	3.02	1.81	4.83
$\text{Al}_{12}\text{Zn}^a$	$\text{C}_1$	$^1\text{A}$	6.66	2.83	1.91	4.74
$\text{Al}_{13}$	$\text{C}_1$	$^2\text{A}$	6.89	3.10	1.89	5.00

**Figure 4.** The total and partial density of states (TDOS, PDOS) for  $\text{Al}_{12}\text{M}$  ( $\text{M}=\text{Cu}, \text{Zn}$ ) clusters. Vertical dashed line corresponds to the HOMO energy level.



To get insight into the electronic properties of the clusters, the total density of states (TDOS) for  $\text{Al}_{12}\text{M}$  ( $\text{M}=\text{Cu}, \text{Zn}$ ) clusters are depicted in Figure 4. For  $\text{M}=\text{Cu}$ , the PDOS show deeper hybridization for the Cu atom, on the other hand for  $\text{M}=\text{Zn}$ , more states near the HOMO energy are found, suggesting that the former ( $\text{Al}_{12}\text{Cu}$ ) is more stable. This preliminary results help for further exploring the reactivity of the clusters, with possible applications in catalysis. [25, 28–32]

## Conclusions

In this preprint, the structural and electronic properties of  $\text{Al}_{12}\text{M}$  ( $\text{Zn}, \text{Cu}$ ) clusters were investigated using density functional theory (DFT) calculations. The results showed that the clusters favor the low-spin states by considering three different functionals, the PBE, PBE0, and TPSSH respectively. The doped clusters showed lower ionization energy and electron affinity compared to the neutral  $\text{Al}_{13}$  cluster. The density of states showed a higher degree of hybridization in  $\text{Al}_{12}\text{Cu}$  compared to  $\text{Al}_{12}\text{Zn}$ .

## Acknowledgments

P.L.R.-K. would like to thank the support of CIMAT Supercomputing Laboratories of Guanajuato and Puerto Interior.

## References

1. J. Graetz, J. Reilly, V. Yartys, J. Maehlen, B. Bulychev, V. Antonov, B. Tarasov, and I. Gabis, “Aluminum hydride as a hydrogen and energy storage material: Past, present and future,” *Journal of Alloys and Compounds*, vol. 509, pp. S517–S528, 2011. Proceedings of the 12th International Symposium on Metal-Hydrogen Systems, Fundamentals and Applications (MH2010).
2. A. Züttel, P. Wenger, S. Rentsch, P. Sudan, P. Mauron, and C. Emmenegger, “ $\text{LiBH}_4$  a new hydrogen storage material,” *Journal of Power Sources*, vol. 118, no. 1, pp. 1–7, 2003. Scientific Advances in Fuel Cell Systems.
3. B. Bogdanović, U. Eberle, M. Felderhoff, and F. Schüth, “Complex aluminum hydrides,” *Scripta Materialia*, vol. 56, no. 10, pp. 813–816, 2007. Viewpoint set no. 42 “Nanoscale materials for hydrogen storage”.

- 
4. L.-P. Tan, D. Die, and B.-X. Zheng, "Growth mechanism, electronic properties and spectra of aluminum clusters," *Spectrochimica Acta Part A: Molecular and Biomolecular Spectroscopy*, vol. 267, p. 120545, 2022.
  5. J. Akola, M. Manninen, H. Häkkinen, U. Landman, X. Li, and L.-S. Wang, "Photoelectron spectra of aluminum cluster anions: Temperature effects and ab initio simulations," *Phys. Rev. B*, vol. 60, pp. R11297–R11300, Oct 1999.
  6. A. Aguado and J. M. López, "Structures and stabilities of  $Al_n^+$ ,  $Al_n$ , and  $Al_n^-$  ( $n=13-34$ ) clusters," *The Journal of Chemical Physics*, vol. 130, p. 064704, 02 2009.
  7. A. Varano, D. J. Henry, and I. Yarovsky, "DFT Study of H Adsorption on Magnesium-Doped Aluminum Clusters," *The Journal of Physical Chemistry A*, vol. 114, no. 10, pp. 3602–3608, 2010. PMID: 20163101.
  8. J. Vanbuel, M.-y. Jia, P. Ferrari, S. Gewinner, W. Schöllkopf, M. T. Nguyen, A. Fielicke, and E. Janssens, "Competitive molecular and dissociative hydrogen chemisorption on size selected doubly rhodium doped aluminum clusters," *Topics in Catalysis*, vol. 61, pp. 62–70, Mar 2018.
  9. S. Das, S. Pal, and S. Krishnamurty, "Dinitrogen activation by silicon and phosphorus doped aluminum clusters," *The Journal of Physical Chemistry C*, vol. 118, pp. 19869–19878, Aug 2014.
  10. C. P. S. Nikhil S. Samudre and S. Krishnamurty, "Understanding the thermal stability of a 3d, 4d, and 5d element doped aluminium nanocluster through bond simulations," *Molecular Simulation*, vol. 49, no. 3, pp. 245–250, 2023.
  11. F. Neese, F. Wennmohs, U. Becker, and C. Riplinger, "The ORCA quantum chemistry program package," *The Journal of Chemical Physics*, vol. 152, p. 224108, 06 2020.
  12. J. P. Perdew, K. Burke, and M. Ernzerhof, "Generalized gradient approximation made simple," *Phys. Rev. Lett.*, vol. 77, pp. 3865–3868, Oct 1996.
  13. J. Tao, J. P. Perdew, V. N. Staroverov, and G. E. Scuseria, "Climbing the density functional ladder: Nonempirical meta-generalized gradient approximation designed for molecules and solids," *Phys. Rev. Lett.*, vol. 91, p. 146401, Sep 2003.
  14. C. Adamo and V. Barone, "Toward reliable density functional methods without adjustable parameters: The PBE0 model," *The Journal of Chemical Physics*, vol. 110, pp. 6158–6170, 04 1999.
  15. F. Weigend and R. Ahlrichs, "Balanced basis sets of split valence, triple zeta valence and quadruple zeta valence quality for h to rn: Design and assessment of accuracy," *Phys. Chem. Chem. Phys.*, vol. 7, pp. 3297–3305, 2005.
  16. T. Lu and F. Chen, "Multiwfn: A multifunctional wavefunction analyzer," *Journal of Computational Chemistry*, vol. 33, no. 5, pp. 580–592, 2012.
  17. P. L. Rodríguez-Kessler, "On the structures and stabilities of  $B_7Cr_2$  clusters: A DFT study," 2024.
  18. P. L. Rodríguez-Kessler, "Revisiting the Global Minimum Structure of the  $Pt_5V$  Cluster," 2024.

- 
19. J. M. Guevara-Vela, M. Gallegos, T. Rocha-Rinza, A. Muñoz-Castro, P. L. Rodríguez-Kessler, and Á. Martín Pendás, "New global minimum conformers for the Pt<sub>19</sub> and Pt<sub>20</sub> clusters: low symmetric species featuring different active sites," *Journal of Molecular Modeling*, vol. 30, p. 310, Aug 2024.
  20. P. Rodríguez-Kessler, A. Vásquez-Espinal, A. Rodríguez-Domínguez, J. Cabellos-Quiroz, and A. Muñoz-Castro, "Structures of Ni-doped Bn (n=1–13) clusters: A computational study," *Inorganica Chimica Acta*, vol. 568, p. 122062, 2024.
  21. P. Rodríguez-Kessler, A. Vásquez-Espinal, and A. Muñoz-Castro, "Structure and stability of Cu-doped Bn (n=1–12) clusters: DFT calculations," *Polyhedron*, vol. 243, p. 116538, 2023.
  22. P. Rodríguez-Kessler and A. Muñoz-Castro, "Structure and stability of Mo-doped Cun (n=1-12) clusters: DFT calculations," *Inorganica Chimica Acta*, vol. 556, p. 121620, 2023.
  23. P. L. Rodríguez-Kessler, A. R. Rodríguez-Domínguez, and A. Muñoz-Castro, "Structural Evolution and Electronic Properties of Intermediate Sized Ti<sub>n</sub> (n=33–60) Clusters," *Advanced Theory and Simulations*, vol. 4, no. 12, p. 2100283, 2021.
  24. P. L. Rodríguez-Kessler, A. R. Rodríguez-Domínguez, D. MacLeod Carey, and A. Muñoz-Castro, "Structural characterization, reactivity, and vibrational properties of silver clusters: a new global minimum for Ag<sub>16</sub>," *Phys. Chem. Chem. Phys.*, vol. 22, pp. 27255–27262, 2020.
  25. P. L. Rodríguez-Kessler, A. Muñoz-Castro, A. R. Rodríguez-Domínguez, and J. L. Cabellos, "Structure effects of Pt<sub>15</sub> clusters for the oxygen reduction reaction: first-principles calculations," *Phys. Chem. Chem. Phys.*, vol. 25, pp. 4764–4772, 2023.
  26. P. L. Rodríguez-Kessler, A. R. Rodríguez-Domínguez, and A. Muñoz-Castro, "On the structure and reactivity of Pt<sub>n</sub>Cu<sub>n</sub> (n=1-7) alloy clusters," *Phys. Chem. Chem. Phys.*, vol. 23, pp. 7233–7239, 2021.
  27. P. Rodríguez-Kessler, A. Muñoz-Castro, P. Alonso-Dávila, F. Aguilera-Granja, and A. Rodríguez-Domínguez, "Structural, electronic and catalytic properties of bimetallic PtnAgn (n=1-7) clusters," *Journal of Alloys and Compounds*, vol. 845, p. 155897, 2020.
  28. P. L. Rodríguez-Kessler and A. R. Rodríguez-Domínguez, "Size and structure effects of PtN (N=12-13) clusters for the oxygen reduction reaction: First-principles calculations," *The Journal of Chemical Physics*, vol. 143, p. 184312, 11 2015.
  29. P. Rodríguez-Kessler, F. Murillo, A. Rodríguez-Domínguez, P. Navarro-Santos, and G. Merino, "Structure of V-doped Pdn (n = 2–12) clusters and their ability for H<sub>2</sub> dissociation," *International Journal of Hydrogen Energy*, vol. 43, no. 45, pp. 20636–20644, 2018.
  30. S. Rodríguez-Carrera, P. Rodríguez-Kessler, F. Ambriz-Vargas, R. Garza-Hernández, R. Reséndiz-Ramírez, J. Martínez-Flores, A. Benitez-Lara, M. Martínez-Gamez, and A. Muñoz-Castro, "First principles study for Ag-based core-shell nanoclusters with 3d-5d transition metal cores for the oxygen reduction reaction," *Inorganica Chimica Acta*, vol. 572, p. 122301, 2024.
  31. D. Olalde-López, P. Rodríguez-Kessler, S. Rodríguez-Carrera, and A. Muñoz-Castro, "Hydrogen storage properties for bimetallic doped boron clusters M<sub>2</sub>B<sub>7</sub> (M=Fe, Co, Ni)," *International Journal of Hydrogen Energy*, 2024.

- 
32. G. Jana, S. Pan, P. L. Rodríguez-Kessler, G. Merino, and P. K. Chattaraj, “Adsorption of molecular hydrogen on lithium–phosphorus double-helices,” *The Journal of Physical Chemistry C*, vol. 122, no. 49, pp. 27941–27946, 2018.